RSC Advances

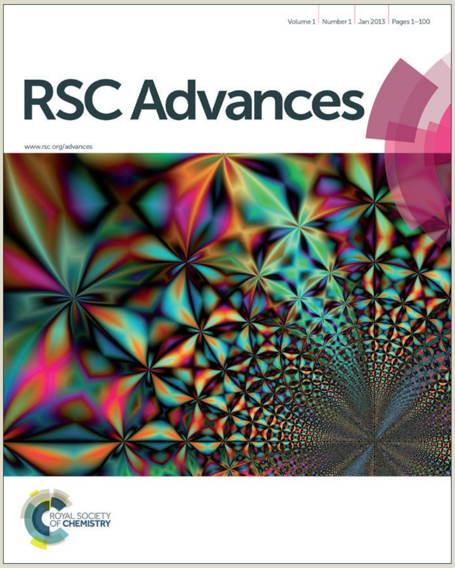

ROYAL SOCIETY OF CHEMISTRY

www.rsc.org/advances

RSC Advances

ARTICLE

# Direct hydroxylation of benzene to phenol with molecular oxygen over vanadium oxide nanosphere and mechanism research

Received 00th January 20xx,
Accepted 00th January 20xx

DOI: 10.1039/x0xx00000x

**www.rsc.org/**

Guanhua Luo[a], Xuechuan Lv[a], Xingwang Wang[ad], Su Yan[a], Xiaohan Gao*[ab], Jie Xu*[c], Hong Ma[c], Yujuan Jiao[a], Fayun Li*[b], Jinzhu Chen[e]

Direct hydroxylation of benzene to phenol using molecular oxygen is a green route with high atom economy but still a great challenge when compared with the existing method of production. The activation of oxygen is necessary and reductive agents were used to activate dioxygen in a so-called “reductive activation” process. Here, nano vanadium oxides that consist mainly of the low valence vanadium to activate dioxygen were prepared in the different condition via hydrothermal method. Under the optimized conditions, an excellent phenol selectivity of 96.3% with benzene conversion of 4.2% was achieved over the $VOC_2O_4$-N-5 without reductive agents. Characterizations revealed that $VOC_2O_4$-N-5 was composed of the mesoporous nanosphere structure with medium strong acid sites and low valence vanadium species. Mechanism was proposed as following: dioxygen was activated by low valence vanadium in $VOC_2O_4$-N-5 to produce the active oxygen species which oxidized acetic acid to peracetic acid. Then the active oxygen species was subsequently transferred from peracetic acid to benzene and inserted into the C-H bond to give phenol.

## 1. Introduction

Direct functionalization of C–H bonds has been recognized as a powerful strategy to form new chemical bonds[1-3]. Many new compounds are produced from the functionalization of C–H bonds. It is so important that the functionalization of C–H bonds is called the “Holy Grails”[4]. In the past decades, the numerous significant developments have been reported. Whereas the one-step hydroxylation of $C_{sp2}$–H bonds still remains a very challenging task because of the conjugated effect[5,6]. Selective oxidation of inert hydrocarbons to industrially important intermediates remains a major challenge[7-10]. For example, the direct hydroxylation of benzene to phenol is considered as one of the top 10 hard issues in the modern chemistry field[11].

Phenol is one of the most important and versatile intermediates of the chemical industry for the manufacture of petrochemicals, agrochemicals and plastics and so on[11-14]. Globally, more than 95% of phenol is produced via the cumene process which is, however, highly energy-consuming, with a low phenol yield and quantitative amount of acetone as a by-product[15]. It is desirable and necessary to synthesize phenol from benzene via one-step approach from the point of view of economy and environment. Various oxidizing agents including $N_2O$[16-18], $H_2O_2$[19-21], $O_2$[22-24], $H_2/O_2$[25,26], air/CO[27], etc were reported for this important transformation. However, the direct oxidation of benzene to phenol using molecular oxygen would be of great potential for industrial application, particularly as it proceeds as a green process[28] (Scheme.1).

The activation of oxygen is a key step for the selective oxidation of benzene to phenol because that the bond energy of the C–H bond of benzene is about 472.2 KJ/mol[29], which is much higher than that of other kinds of C–H bond. Therefore, the the C–H bond in benzene is difficult to be activated. The active oxygen species is produced from molecular oxygen by the reducing reagent in

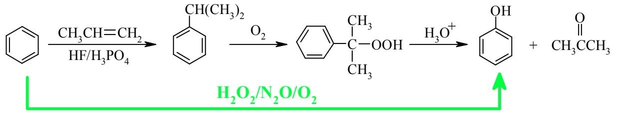

---

[a] School of Chemistry and Material Science, College of Chemistry, Chemical Engineering and Environmental Engineering, Liaoning Shihua University, Liaoning Fushun 113001, China.

[b] Institute of ecological environment, College of Chemistry, Chemical Engineering and Environmental Engineering, Liaoning Shihua University, Liaoning Fushun 113001, China.

[c] Dalian National Lab for Clean Energy, State Key Laboratory of Catalysis, Dalian Institute of Chemical Physics, Chinese Academy of Sciences, Dalian 116023, People Republic of China.

[d] China Petroleum Engineering(CPE), Beijing 100083, China.

[e] CAS Key Laboratory of Renewable Energy, Guangzhou Institute of Energy Conversion, Chinese Academy of Sciences, Guangzhou 510640, P. R. China.

Scheme.1 Route of phenol production

a so-called “reductive activation” process[30]. In our pervious papers[28. 31. 32], we had proved that the oxygen can be activated by low valence vanadium species. The similar catalysts were proved to be reused and the vanadium value of the fresh and used catalyst was studied. Whereas the transfer process of the active oxygen species is still unclear and the influencing factors on the catalyst performance need more research.

In this paper, we reported the direct hydroxylation of benzene with molecular oxygen to phenol catalyzed by the nano vanadium oxide. Nano vanadium oxides were prepared in the various conditions using aniline as the template and reducing agent to achieve the low valence vanadium species. The effects of the prepared condition of the catalysts on its catalytic performance were discussed in detail. The optimized catalyst was fully characterized to investigate the structure, properties and the vanadium valence of the catalyst. The transfer process of the active oxygen species was studied by the real-time in situ infrared spectra measurements.

## 2. Results and discussion

### 2.1. Influence of preparation conditions on the performance of catalysts

In this research, vanadium pentoxide and vanadyl oxalate were selected as vanadium source with aniline as the template and reducing agent, the resulted nano vanadium oxide was investigated as potential redox catalyst for direct hydroxylation of benzene to phenol with molecular oxygen. The preparation conditions of catalyst would affect the structure, properties and valence of active site of the catalyst, which, as a result, are closely associated with the catalytic performance. The influences of the prepared conditions, such as vanadium source, aging time and ratio of vanadium to aniline, on the performance of catalysts were displayed in Table. 1. Initially, vanadium pentoxide was selected as vanadium source with the molar ratio of vanadium to aniline of 1:1 and the aging time of 1 h, excellent phenol selectivity of 90.5% was achieved with benzene conversion of 3.1% (Table. 1, Entry 1). Further increase of aging time of decrease of the molar ratio of vanadium to aniline, however, led to a slight drop in phenol yields (Table. 1, Entries 2-6). It is well known that vanadium pentoxide is insoluble in water. Consequently, vanadyl oxalate ($VOC_2O_4$) was selected as the soluble vanadium source to completely react with aniline. Notably, excellent benzene conversion as well as phenol selectivity was observed over the vanadyl oxalate-derived catalyst with phenol yield of 3.5% (Table. 1, Entry 7).

### 2.2. Influence of the volume ratio of ethanol to water on the catalyst performance

In order to make vanadyl oxalate and aniline react completely, ethanol was added to dissolve aniline in water. Influence of the volume ratio of ethanol to water on the catalyst performance was illuminated in Fig. 1. It can be seen that the selectivity of phenol increases with the amount of ethanol addition. Notably, the $VOC_2O_4$-N-5 catalyst, made of the volume ratio of ethanol to water of 4, exhibited remarkable catalytic performance, producing benzene conversion of 4.2% with phenol selectivity of 96.3%.

Table. 1 Influence of prepared conditions on the performance of catalysts

| Entry | Vanadium source | Aging time | Vanadium/ Aniline(mol) | Conversion of benzene (%) | Selectivity of phenol (%) | Yield of phenol(%) |
|---|---|---|---|---|---|---|
| 1 | $V_2O_5$ | 1 h | 1:1 | 3.1 | 90.6 | 2.8 |
| 2 | $V_2O_5$ | 1 h | 1:2.5 | 2.7 | 85.7 | 2.3 |
| 3 | $V_2O_5$ | 1 h | 1:5 | 2.8 | 88.6 | 2.5 |
| 4 | $V_2O_5$ | 48 h | 1:1 | 2.8 | 91.0 | 2.5 |
| 5 | $V_2O_5$ | 48 h | 1:2.5 | 3.1 | 86.2 | 2.7 |
| 6 | $V_2O_5$ | 48 h | 1:5 | 2.5 | 89.5 | 2.2 |
| 7 | $VOC_2O_4$ | 1 h | 1:1 | 3.8 | 94.0 | 3.5 |

RSC Advances

ARTICLE

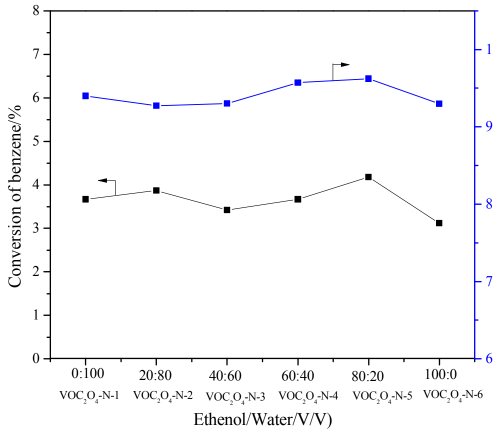

**Fig. 1** Influence of the volume ratio of ethanol to water on catalyst performance.

### 2.3 Performances of recycling VOC$_2$O$_4$-N-5

Recycle test performance is one of the important characters of catalysts. The used VOC$_2$O$_4$-N-5 catalyst was separated by filtration and washed with copious amounts of water every time. Fig. 2 is the reusability test of the VOC$_2$O$_4$-N-5 catalyst. The activity of VOC$_2$O$_4$-N-5 catalyst changed a little that benzene conversion is about 4.15% form first run to forth run. In the fifth run, the conversion of benzene dropped to 3.9%. The reason may be that some of the active centers of the catalyst may be leach out or become inactive. However, the selectivity of phenol remained in the recycle test. The recycling test confirmed that the catalyst is reusable.

### 2.4. XRD analysis

The crystal structure of catalysts prepared in the mixture solution of ethanol to water was studied by XRD and the results were showed in Fig. 3. The diffraction peaks at 2θ=24.42, 31.18 35.56, 41.58 and 54.56° appeared in all catalysts. In fact, the above peaks were also detected in VOC$_2$O$_4$-N-5 after a magnified observation. Whereas the intensity of these peaks are weak and FWHM (Full Width at Half Maximum) is broad, which indicated that the crystallinity of catalysts is poor and the granularity is big. These diffraction peaks can be indexed to monoclinic phase VO$_2$ (pdf. No.74-1642) and rhombohedral phase V$_2$O$_3$ (pdf. No.84-0319). Diffraction peak at 2θ=19.1° appeared in curves of VOC$_2$O$_4$-N-1, VOC$_2$O$_4$-N-2 and VOC$_2$O$_4$-N-4 was indexed to monoclinic phase V$_3$O$_8$H$_4$ (pdf. No.72-1229). Diffraction peak at 2θ=18.4° appeared in curves of VOC$_2$O$_4$-N-3, VOC$_2$O$_4$-N-4 and VOC$_2$O$_4$-N-6 was indexed to monoclinic phase H$_6$V$_4$O$_{10}$ (pdf. No.41-495). Diffraction peak at 2θ=7.5° appeared in curves of VOC$_2$O$_4$-N-1 and VOC$_2$O$_4$-N-4 was indexed to monoclinic phase V$_5$O$_{12}$ 5H$_2$O (pdf. No.45-1401). A strong and sharp peak appeared at 2θ=10.88° in VOC$_2$O$_4$-N-5 was indexed to monoclinic phase (NH$_4$)$_2$V$_6$O$_{16}$·1.5H$_2$O (pdf. No.51-0376). XRD analysis results indicated that all the catalysts consist of low valence vanadium oxide which is in accordance with the purpose of the catalyst preparation. Therefore the catalysts possess outstanding catalytic activity. Whenas, some pentavalent vanadium species existed in the VOC$_2$O$_4$-N-5 catalyst and VOC$_2$O$_4$-N-5 showed excellent performance. The reason may be that the catalytic cycle was easily formed between pentavalent vanadium species and low valence vanadium species. Dioxygen was reductive activated by low valence vanadium species and low valence vanadium species was oxidized to pentavalent vanadium species. The pentavalent vanadium species existed beforehand was reduced to low valence vanadium species in some way. Then the catalytic cycle was easily formed in the VOC$_2$O$_4$-N-5 catalyst.

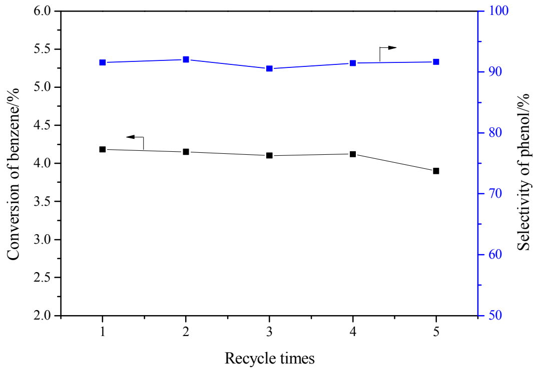

**Fig. 2** Performances of recycling VOC$_2$O$_4$-N-5.

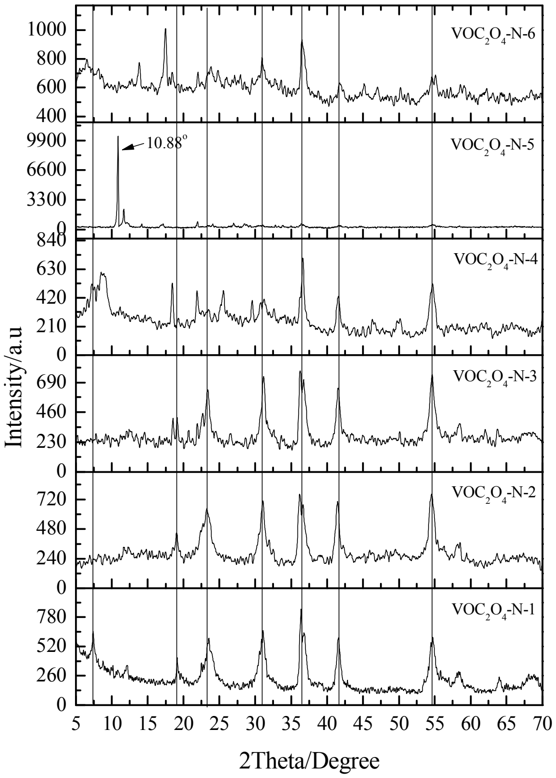

**Fig. 3** XRD patterns of the catalysts prepared in the mixture solution of ethanol to water.

Combination of XRD analysis and influence of the volume ratio of ethanol to water on the catalyst performance illuminated that the volume ratio of ethanol to water had an important effect of the crystal structure of catalysts which is closely associated with the catalytic performance. When the volume ratio of ethanol to water is 4, monoclinic phase $(NH_4)_2V_6O_{16}\cdot1.5H_2O$ was formed in the $VOC_2O_4$-N-5 catalyst that benefited the catalytic cycle formation. Therefore $VOC_2O_4$-N-5 achieved phenol selectivity of 96.3% with benzene conversion of 4.2%.

### 2.5. SEM images

Fig. 4 showed the SEM images of the catalyst samples. $VOC_2O_4$-N-1 catalyst consisted of the irregular nanosheet with sheet thickness about 20~30 nm. The SEM micrographs of $VOC_2O_4$-N-2, $VOC_2O_4$-N-3, $VOC_2O_4$-N-4 and $VOC_2O_4$-N-6 present the different morphologies and sizes block. SEM analysis of VOC2O4-N-5 revealed that it is composed of uniform and regular spherical

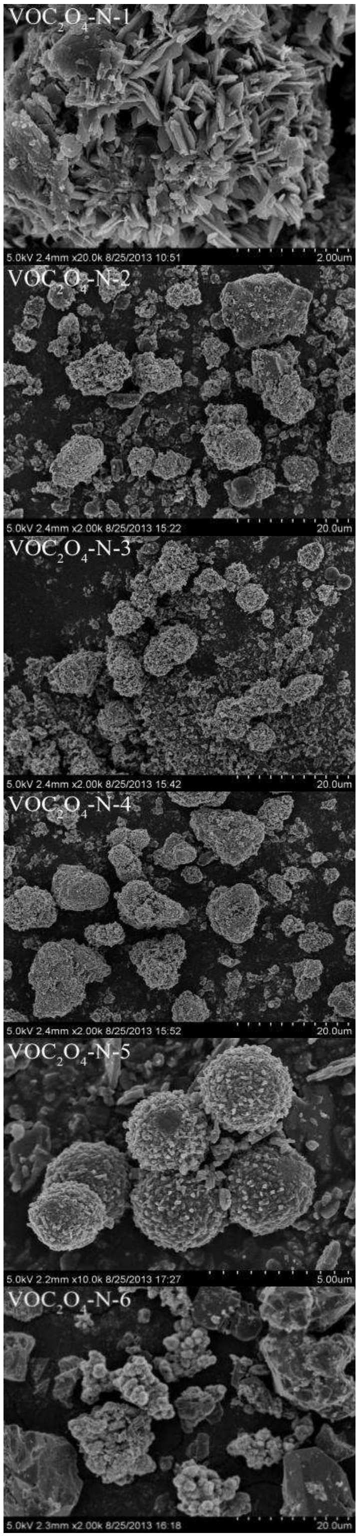

**Fig. 4** SEM images of the catalysts prepared in the mixture solution of ethanol to water.

nanoparticles with the dimension of 500~1000 nm and rough surface structure. The results of SEM images are in line with that of XRD analysis. Nanosheets were generally formed in pure water. The reason may be that vanadyl oxalate dissolved in water, whereas aniline could not dissolved in water. $VO^{2+}$ and aniline absorbed each other to rearrange to form the sheet. As ethanol volume was added, aniline was dissolved in mixture. $VO^{2+}$ and aniline polymerized to form the block, whereas the crystal structure of $VOC_2O_4$-N-1 is similar to others. When the volume ratio of ethanol to water is 80:20, nanosphere created because new crystal phase emerged.

### 2.6. TG analysis of $VOC_2O_4$-N-5

TG analysis for $VOC_2O_4$-N-5 under air or nitrogen atmosphere is shown in Fig. 5. A weight loss of 6.0% below 180 °C is associated with the release of the adsorbent water. A further mass loss of 2.0% observed in the temperature range from 190 to 290 °C is assigned to the decomposition and loss of the crystalliferous water. Subsequent mass loss of 2.0% between 290 and 355 °C is considered as the decomposition of the residual organic compound. The weight is unchanged under nitrogen atmosphere after 355 °C. But a weight increase about 1.0% was observed under air atmosphere after 355 °C which is attributed to the oxidation of low valence vanadium species in the catalyst under air atmosphere. TG curves of $VOC_2O_4$-N-5 illuminated that the catalyst is stable under the reaction temperature.

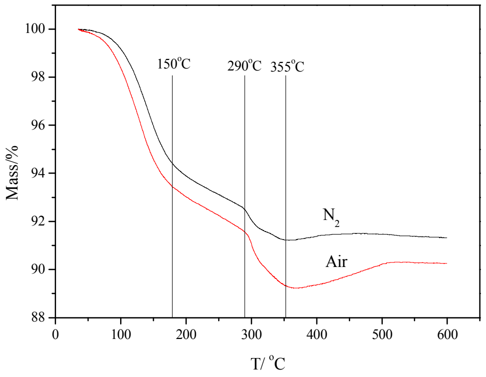

**Fig. 5** TG curve for $VOC_2O_4$-N-5.

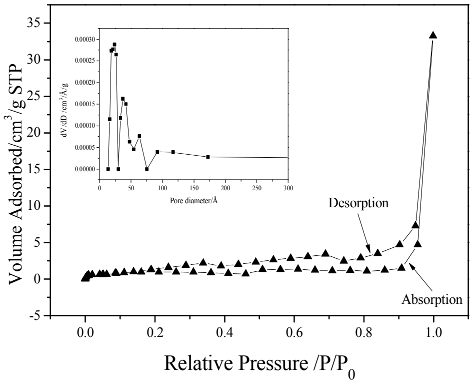

**Fig. 6** $N_2$ absorption-desorption isotherms and pore distribution profiles for $VOC_2O_4$-N-5.

### 2.7. $N_2$ absorption-desorption isotherms of $VOC_2O_4$-N-5

$N_2$ adsorption–desorption isotherms and pore distribution profiles of $VOC_2O_4$-N-5 are given in Fig. 6. The samples exhibit type IV isotherms (defined by IUPAC) with small hysteresis[33], which is characteristic for mesoporous materials. The nitrogen sorption study showed that the BET surface area of $VOC_2O_4$-N-5 is 3.7 $m^2{\cdot}g^{-1}$ and the mesopore volume is 1.26 $cm^3{\cdot}g^{-1}$. The average pore diameter is calculated to be 3.8 nm using the BJH method. The surface area of $VOC_2O_4$-N-5 is small and the pore size distribution is wide. How to prepare the catalyst possessing large specific surface area and uniform pore size that is benefit for the catalytic performance is the goal of the future work.

### 2.8. $NH_3$-TPD of $VOC_2O_4$-N-5

Fig. 7 is the $NH_3$-TPD profiles for $VOC_2O_4$-N-5 to investigate the surface acid amount and acid strength. There are two desorption peaks appeared at 195 °C and 341 °C in the curve of sample. The major peak at 341 °C is assigned to the medium strong acid sites that may be the active center. There is an isolated electron pair at O atom of the dioxygen that could think as alkali. Dioxygen could be adsorbed by the acid sites of $VOC_2O_4$-N-5 catalyst to be activated. It is well known that benzene is a planar, cyclic compound with two cyclic clouds of delocalized electrons. Because its $\pi$ electrons are delocalized and abundant, then benzene could act as alkali which could produce the adsorption with acid. Therefore, the acid sites of $VOC_2O_4$-N-5 catalyst could adsorbed benzene and activate the C-H bond of benzene to benefit the insertion of the active oxygen species.

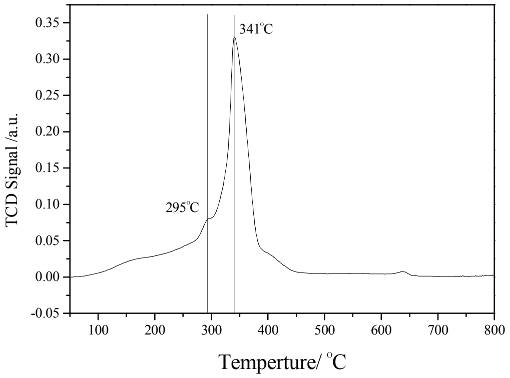

**Fig. 7** $NH_3$-TPD for $VOC_2O_4$-N-5.

### 2.9. Real-time in situ FTIR for the catalytic system[34-36]

The active oxygen species transmission and mechanism were studied through the real-time in situ Fourier transform infrared (FTIR) spectral measurements and the corresponding results are listed in Fig. 8. Before the addition of dioxygen near the reaction temperature, backgrounds (catalyst, solvent and benzene) were corrected. The probes began scanning after the dioxygen addition and the spectra were obtained every 20 minutes. It could be seen from the Fig. 8. that the bands emerged at 1722, 1350~1600, 890, 753 and 690 $cm^{-1}$ and have noticeable changes as the reaction proceed. The bands at 1350~1600 $cm^{-1}$ were assigned as the breathing vibration of the C=C in the benzene ring. The 753 and 690 $cm^{-1}$ bands are related the out-of-plane bending of the C-H for the one substituted benzene, indicating the formation of phenol. The absorption band at 890 $cm^{-1}$ was ascribed to the out-of-plane bending of the O-H bond in phenol. The band around 1650~1750 $cm^{-1}$ is an assignment of the characteristic peaks of C=O stretching vibration. Band appeared at 1722 $cm^{-1}$ indicated the formation of new compound containing C=O bond. Acetic acid is the sole compound contained C=O bond with the FTIR absorption band at 1714 $cm^{-1}$. It was proposed that acetic acid is oxidized to peracetic acid and the slight shift from 1714 to 1722 $cm^{-1}$ is attributed to the effect of the peroxide bond. In addition, the intensity of the bands at 1350~1600, 890, 753 and 690 $cm^{-1}$ were weak at the beginning and became stronger as time increased. These results suggested that the formation rate of phenol is slow initially and is significantly improved after one hour then keeps steadily after that time. Whereas, the intensity of the band emerged at 1722 $cm^{-1}$ increased quickly at the first and decreased slowly. The phenomenon indicated that peracetic acid generated quickly upon exposure to dioxygen and consumed with the phenol formation.

Therefore, the mechanism for the direct hydroxylation of benzene into phenol using dioxygen was proposed as following (Scheme.2): the low valence vanadium species activated dioxygen to produce the active oxygen species [$O_2^{-}\cdot$] and low valence vanadium species was oxidized to pentavalent vanadium species. Disproportionation reaction of [$O_2^{-}\cdot$] easily occurred. One is oxidation reaction of acetic acid to peracetic acid. Another is reduction reaction of pentavalent vanadium species to low valence vanadium species that the catalytic cycle was formed. Then the active oxygen species was transferred from peracetic acid to the C-H bond of benzene that is adsorbed and activated by the acid sites of $VOC_2O_4$-N-5 catalyst to produce phenol.

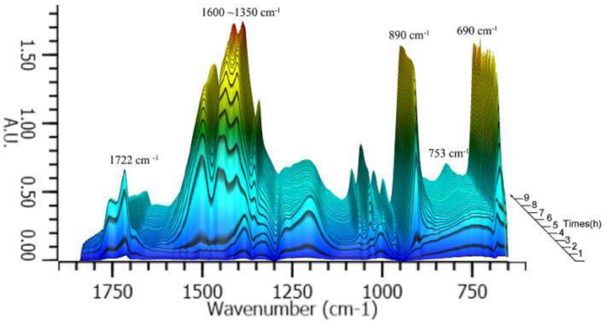

**Fig. 8** Real-time in situ FTIR for the catalytic system.

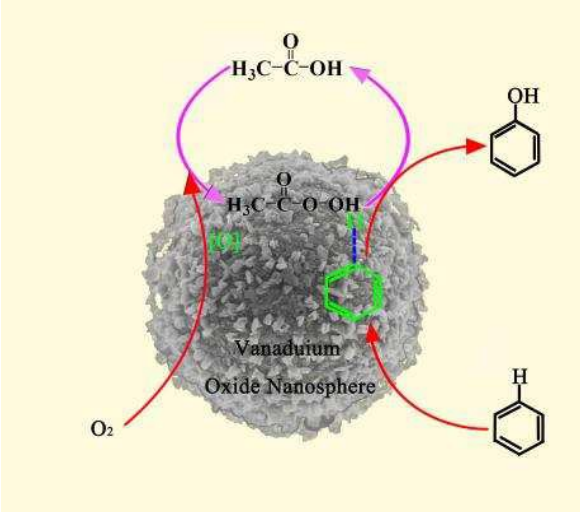

Scheme.2 Proposed mechanism

## 3. Expermental

### 3. 1. Catalyst preparation

Vanadium source is vanadium pentoxide, the preparation procedure was as follows: the different molar ratio of $V_2O_5$ to aniline were mixed with 100 mL distilled water. After vigorous stirring and aging for 1 h or 48 h, a yellow composite of the organic template and the vanadium oxide component was obtained. The composite was treated hydrothermally in a Teflon-lined autoclave with a stainless steel shell at 140 °C for 24 h, and then at 180 °C for 3 days. The obtained black product was washed with distilled water and ethanol to remove the unreacted amine and decomposition products, and finally dried at 70 °C in an air atmosphere for 6 h.

Vanadium source is vanadyl oxalate, the prepared procedure is as follows: vanadyl oxalate is synthesized form vanadium pentoxide and oxalic acid in the distilled water a day ahead. Aniline was mixed with solvent that is the mixture solvent of distilled water and ethanol at different ratio. Then the solution containing vanadyl oxalate was added into the solution containing aniline slowly through the separalory funnel. The stirring and aging time is 1 h. The following procedure is as same as the above. The total volume of solvent is 100 mL. The volume ratio of ethanol to water is 0:100, 20:80, 40:60, 60:40, 80:20 and 100:0. The corresponding catalysts were assigned to $VOC_2O_4$-N-1, $VOC_2O_4$-N-2, $VOC_2O_4$-N-3, $VOC_2O_4$-N-4, $VOC_2O_4$-N-5, and $VOC_2O_4$-N-6 respectively.

### 3.2. Oxidation reaction and products analysis

The liquid-phase oxidation of benzene to phenol with molecular oxygen was performed in a 100 mL Teflon-lined stainless steel reactor with a magnetic stirrer. The standard condition was as follows: 0.10 g catalyst, 1 mL (0.011 mol) benzene and 10 mL acetic acid were added in the reactor and heated. After the temperature was raised to 150 °C, the oxygen was introduced to 1.00 MPa and the consumed oxygen was supplied at any moment. The reactions were carried out at the conditions for 10 h.

The product was analyzed by GC (TECHCOMP 4900) with an HP-5 capillary column (50 m x 0.32 mm x 0.4 μm). Qualitative analysis of phenol, catechol, 1, 4-benzoquinone, biphenyl and hydroquinone in the products was verified by comparison with the retention times of standard samples. The quantitative analysis of the mixture was determined from the calibration curves, using toluene as the internal standard.

All the reagents above were analytical reagent.

### 3.3. Catalyst characterization

The TG measurement of the sample was carried out by a thermogravimetric analyzer (Model: DT-20B, Shimadzu, Japan) at the heating rate of 10 °C /min under air or nitrogen atmosphere with flow rate of 30 mL/ min.

Powder X-ray diffraction (XRD) patterns were recorded using Rigaku D/Max 3400 X with Cu Kα radiation at 0.02 steps per second in angle range $2\theta = 5\text{-}90^{\circ}$.

Scanning electron microscopy (SEM) image was collected on a JSM-6360LV microscope.

Low-temperature $N_2$ adsorption–desorption experiments were carried out using a Quantachrome Autosorb-1 system. The modal pore diameter was calculated using the BJH method based on the desorption isotherm, and the surface area was calculated using the BET method based on the adsorption isotherm.

$NH_3$-TPD (temperature-programmed desorption) experiments were performed using Micromeritics Instrument Corporation -- AutoChem II 2920.

Real-time in situ infrared spectra measurements were carried out on a Mettler toledo ReactIR$^{TM}$ 45 m equipped with an external AgX fiber conduit diamond ATR probe. The experiment was carried out in Dalian Institute of Chemical Physics, Chinese Academy of Sciences.

## 4. Conclusions

In summary, nano vanadium oxides were prepared by hydrothermal synthesis under various conditions and were fully characterized. The optimized conditions to prepare catalyst is that the molar ratio of vanadium to aniline is 1:1 with 1 h aging time, vanadyl oxalate as vanadium source and the volume ratio of ethanol to water of 4. Characterizations revealed that $VOC_2O_4$-N-5 is composed of low valence vanadium species and mesoporous nanosphere structure with the medium strong acid sites. The $VOC_2O_4$-N-5 catalyst exhibited high catalytic activity for hydroxylation reaction of benzene and dioxygen to afford phenol without using reduced reagent. Excellent phenol selectivity of 96.3% with benzene conversion of 4.2% was obtained over $VOC_2O_4$-N-5 catalyst under the investigated conditions.

Reaction mechanism was investigated through the real-time in situ Fourier transform infrared (FTIR) spectral measurement. The results indicated that the active oxygen species [$O_2^-\cdot$] was produced from dioxygen activated by the low valence vanadium species of the $VOC_2O_4$-N-5. Pentavalent vanadium species was reduced to low valence vanadium species and acetic acid was oxidized to peracetic acid due to the dismutation reaction of the active oxygen species. Peracetic acid subsequently transferred the active oxygen species to benzene leading to the insertion the activated C-H bond by the acid sites to give phenol.

In spite of the fact that $VOC_2O_4$-N-5 shows better performance, the future issue on the $VOC_2O_4$-N series catalysts is how to prepare the catalyst possessing the large specific surface area, single crystal phase and uniform pore size which closely associated with the catalytic activity.

## Acknowledgements

This work was financially supported by the National Nature Science Foundation of China under the grant NSFC. NO. 21103078, 21003069.

## Notes and References

1 Y. Yan, P. Feng, Q. Z. Zheng, Y. F. Liang, J. F. Lu, Y. Cui and N. Jiao, *Angew. Chem. Int. Ed.*, 2013, **52**, 5827.
2 K. Godula, D. Sames, *Science.*, 2006, **312**, 67.
3 C. Jia, T. Kitamura and Y. Fujiwara, *Acc. Chem. Res.*, 2001, **34**, 633.
4 A. J. Bard, G. M. Whitesides, R. N. Zare and F. W. McLafferty, *Acc. Chem. Res.*, 1995, **28**, 91.
5 S. S. Acharyya, S. Ghosh, N. Siddiqui, L. N. S. Konathala and R. Bal, *RSC. Adv.*, 2015, **5**, 4838.
6 D. Y. Tang, L. F. Zhu and C. W. Hu, *RSC Adv*., 2012, **2**, 2329.
7 S. S. Stahl, *Angew. Chem. Int. Ed.*, 2004, **43**, 3400.
8 J. A. Labinger, J. E. Bercaw, *Nature.*, 2002, **417**, 507.
9 J. M. Thomas, R. Raja, G. Sankar and R. G. Bell, *Nature.*, 1999, **398**, 227.
10 M. Tobisu, N. Chatani, *Angew. Chem. Int. Ed.*, 2006, **45**, 1683.
11 G. I. Panov, *CATTECH.*, 2000, **4**, 18.
12 T. Miyahara, H. Kanzaki, R. Hamada, S. Kuroiwa, S. Nishiyama and S. Tsuruya, *J. Mol. Catal. A: Chem.*, 2001, **176**, 141.
13 N. I. Kuznetsova, L. I. Kuznetsova, V. A. Likholobov and G. P. Pez, *Catal. Today.*, 2005, **99**, 193.
14 D. Xu, L. H. Jia and X. F. Guo, *Catal. Lett.*, 2012, **142**, 1251.
15 A. Conde, M. M. Díaz-Requejo and P. J. Pérez, *Chem. Commun.*, 2011, **47**, 8154.
16 A. Koekkoek, Q. Yang, R. A. van Santen, C. Li, E. J and M. Hensen, *Chem. Commun.*, 2009, **45**, 7590.
17 V. S. Chernyavsky, L. V. Pirutko, A. K. Uriarte, A. S. Kharitonov and G. I. Panov, *J. Catal.*, 2007, **245**, 466.
18 V. I. Sobolev, G. I. Panov, A. S. Kharitonov, V. N. Romannikov, A. M. Volodin and K. G. Ione, *J. Catal.,* 1993, **139**, 435.
19 L. Balducci, D. Bianchi, R. Bortolo, R. D'Aloisio, M. Ricci, R. Tassinari and R. Ungarelli, *Angew. Chem. Int. Ed.*, 2003, **42**, 4937.
20 T. Jiang, W. T. Wang and B. X. Han, *New. J. Chem.*, 2013, **37**, 1654.
21 P. F. Zhang, Y. T. Gong, H. R. Li, Z. R. Chen and Y. Wang, *RSC Adv.*, 2013, **3**, 5121.
22 Y. Y. Gu, X. H. Zhao, G. R. Zhang, H. M. Ding and Y. K. Shan, *Appl. Catal. A: Gen.*, 2007, **328**, 150.
23 Y. Y. Liu, K. Murata and M. Inaba, *Catal. Commun.*, 2005, **6**, 679.
24 W. Laufer, J. P. M. Niederer and W. F. Hoelderich, *Adv. Synth. Catal.*, 2002, **344**, 1084.
25 S. Niwa, M. Eswaramoorthy, J. Nair, A. Raj, N. Itoh, H. Shoji, T. Namba and F. Mizukami, *Science.*, 2002, **295**, 105.
26 N. Itoh, S. Niwa, F. Mizukami, T. Inoue, A. Igarashi and T. Namba, *Catal. Commun.*, 2003, **4**, 243.
27 M. Tani, T. Sakamoto, S. Mita and S. Sakaguch. Y. Ishii, *Angew. Chem. Int. Ed.*, 2005 **44**, 2155.
28 X. H. Gao, X. C. Lv and J. Xu, *Chinese. J. Chem.*, 2009, **27**, 2155.
29 K. M. Ervin, V. F. Deturi, *J. Phys. Chem. A.*, 2002, **106**, 9947.
30 H. Ehrich, H. Berndt, M. M. Pohl, K. Jahnisch and M. Baerns, *Appl. Catal. A.*, 2002, **230**, 271.
31 X. H. Gao, J. Xu, *Catal. Lett.*, 2006, **111**, 203.
32 X. H. Gao, X. C. Lv and J. Xu, *Kinet. Catal.*, 2010, **51**, 394.
33 R. R. Ru, W. Q. Pang (Eds.), *Zeolite and Porous Material Chemistry*, Science Press, Beijing, 2004. p. 145.
34 P. Y. Bruise (Eds.), *Organic Chemistry, sixth ed*, Prentence Hall Press, New York, 2011. p. 518-543.
35 F. A. Carey (Eds.), *Organic Chemistry, fourth ed*, Hill Companies, Inc, New York, 2000. p. 487.
36 Y. X. Zhao, X. Y. Sun (Eds.), *Identification of the Organic Molecular Structure by Spectroscopy, fourth ed*, Science Press, Beijing, 2010. p. 90-139.